
Audio Geolocation: A Natural Sounds Benchmark

Mustafa Chasmai Wuao Liu Subhransu Maji Grant Van Horn

University of Massachusetts Amherst

{mchasmai, wuaoliu, smaji, gvanhorn}@cs.umass.edu

Abstract

Can we determine someone’s geographic location purely from the sounds they hear? Are acoustic signals enough to localize within a country, state, or even city? We tackle the challenge of global-scale audio geolocation, formalize the problem, and conduct an in-depth analysis with wildlife audio from the iNatSounds dataset. Adopting a vision-inspired approach, we convert audio recordings to spectrograms and benchmark existing image geolocation techniques. We hypothesize that species vocalizations offer strong geolocation cues due to their defined geographic ranges and propose an approach that integrates species range prediction with retrieval-based geolocation. We further evaluate whether geolocation improves when analyzing species-rich recordings or when aggregating across spatiotemporal neighborhoods. Finally, we introduce case studies from movies to explore multimodal geolocation using both audio and visual content. Our work highlights the advantages of integrating audio and visual cues, and sets the stage for future research in audio geolocation.

1 Introduction

Image geolocation has been extensively studied in the computer vision community, with methods exploring classification [4, 16, 45, 49, 54, 61, 63], contrastive learning [39, 60] and multimodal representations [70, 73, 74]. The best models can place 40% of images within 25 km of their actual location, rivaling top human geoguessers [29]. In this work, we shift focus to predicting the recording location of audio, addressing the unique challenges of global audio geolocation.

Image geolocation methods look for visual cues like famous landmarks, landscape type, or architectural style to infer location from a random image. Geolocating random audio, however, can be ill-posed, as many sounds are not necessarily associated with a specific geographic location. Early studies [40, 48] focus on urban sounds like jackhammers and traffic noise as signals to geolocate. We hypothesize that wildlife sounds offer another promising signal. Each species has a defined geographic range, and identifying audible species in a recording can help constrain the possible locations. Intuitively, by intersecting range maps of detected species, we can significantly narrow down the search area (Fig. 1). If the detected species have large ranges, then the search area might still involve hundreds or thousands of square kilometers. However, if any of the detected species has a restricted range, the plausible search space might be narrowed down to tens of kilometers.

Our experiments reveal that accurate geolocation is possible if we know *all* species present in a location, and performance improves as species diversity increases. However, identifying audible species with high recall presents its own set of challenges [7, 53]. First, short audio recordings may simply not capture enough of the vocalizing species present at a location. Even for species that are recorded, low signal-to-noise ratio, and fine-grained confusions can further reduce recall. Rare species have unique geographic footprints ideal for geolocation, but identifying these rare species is especially difficult. In this work, we explore these challenges while geolocating audio in iNatSounds [7], a geographically and ecologically diverse natural audio dataset.

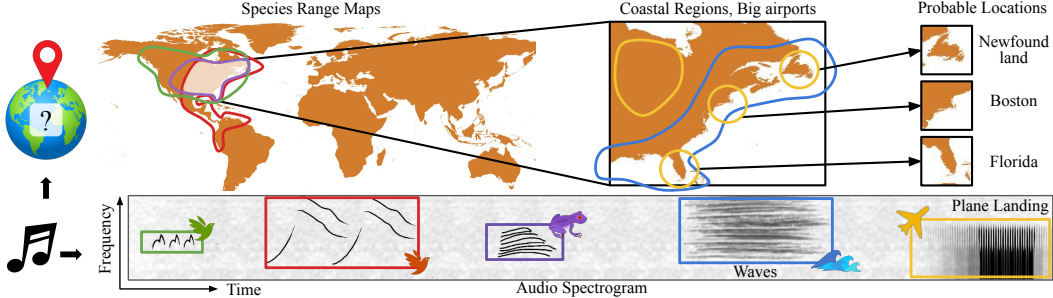


Figure 1: **Intuition for Audio Geolocation.** If a model were to recognize different species’ vocalizations, the intersection of their geographic range maps could help narrow down the location. Ambient sounds like waves or airplane noises could provide additional context to refine the estimate. While our models do not explicitly detect these sound events, we hypothesize that they leverage these types of signals *implicitly* to perform geolocation.

Joint learning of audio and location embeddings is also a common practice in the field of soundscape mapping [2, 37, 38, 52], where the goal is to model the acoustic environment of a location. For example, a busy city intersection may be dominated by traffic noise, whereas a rural farm is more likely to feature natural sounds. While soundscape mapping methods can be indirectly used to geolocate audio too, they cover only a narrow slice of the broader solution space. Other approaches have explored implicit audio-location pairing through intermediate modalities such as images [53], but these too do not directly address the problem of geolocating audio. Audio geolocation presents unique challenges that warrant dedicated investigation. The ability to infer location solely from sound also enables impactful real-world applications like geographic priors [7] and geo-forensics (Fig. 4). In this work, we position audio geolocation as a core research problem and set the stage for future explorations in this space. We release our benchmark [here](#) and codebase [here](#).

We summarize our main contributions as follows:

1. To the best of our knowledge, this is the first study addressing the global-scale geolocation of natural audio. We formalize the audio geolocation problem and extensively benchmark existing image-based geolocation and soundscape mapping methods. Additionally, we propose a novel approach leveraging species range predictions to improve geolocation accuracy, further contextualizing our results through comparisons with geolocation using oracle species information.
2. We investigate whether geolocation improves when using species-rich audio or aggregating recordings from spatiotemporal neighborhoods. To this end, we construct XCDC, a dataset of long dawn chorus recordings from Xeno-Canto [68], and evaluate models that geolocate clusters of iNatSounds [7] recordings sampled from nearby times and locations.
3. We introduce Multimodal Geo-Forensics through case studies of movie audio and imagery, illustrating potential real-world applications of multimodal geolocation.

2 Related Work

Audio Geolocation. The task of explicit geolocation of audio recordings remains largely under-explored. Several early studies [14, 25, 26, 40, 48] investigate audio and multimodal geolocation, but are limited to distinguishing sounds within or among specific regions. Motivated by the growing interest in image geolocation, we revisit and scale up the problem of audio geolocation from a modern perspective, aiming to address it at a global scale. Insights gained from our explorations in natural domains could also contribute to broader advancements in audio geolocation, as wildlife sounds such as birds and insects are also prevalent in urban settings.

Image Geolocation. Initial methods for image geolocation approached the problem through the lens of retrieval. To geolocate a ground image, they retrieved similar geo-tagged ground images [31] or cross-view satellite images [42, 55, 64, 70, 73, 74]. Focus gradually shifted to feed-forward classification models that could directly predict location from an image by splitting the surface of the earth into several geo-cells and predicting the correct geo-cell [4, 16, 45, 49, 54, 61, 63]. To overcome grid resolution constraints, some works explore adaptive grids [54] and hierarchical approaches [16]. Haas et al. [29] incorporate political and administrative boundaries while creating their grids and beat one of the world’s foremost professional GeoGuessr players [27].

Following the release of CLIP [50], recent methods [39, 60] have revisited the retrieval approach. These methods treat the location itself as a modality and learn location embeddings aligned with images. GeoCLIP [60] learns a location encoder that utilizes random Fourier features to capture high frequency details and learn better location features. SatCLIP [39] encodes location via spherical harmonics and learns a joint embedding space with paired satellite images. Zhou et al. [72] propose to leverage LLMs [1, 58] and incorporate domain knowledge with Retrieval Augmented Generation (RAG) [6]. In this work, we also adopt a location retrieval approach inspired by CLIP and systematically evaluate the impact of different audio and location embeddings.

Soundscape Mapping and Audio-Location Alignment. In the acoustic space, researchers are also interested in the complementary problem of soundscape mapping. Instead of identifying geographically unique signals in audio recordings, the focus is to learn common patterns in sounds from a particular location. The task is posed as a retrieval of audio conditioned on location. Prior research focus on understanding the soundscapes of either a few cities [2] or for the entire earth [52]. GeoCLAP [37] and PSM [38] use satellite images to implicitly represent geographic location and learn a shared embedding space between overhead images and ground audio. The domain of wildlife sounds also provides a unique set of challenges not as prominent in urban settings. Taxabind [53] learns a shared feature space for 6 modalities related to species and demonstrate its benefit to ecological problems. However, they too do not focus on audio geolocation and have *implicit* audio-location pairing with ground images as an intermediary. While these methods can be implicitly used for geolocation, the unique challenges of global audio geolocation remain largely underexplored.

Related Audio Tasks. In acoustic analysis, prior work [15, 19, 41, 56, 66, 71] also focus on localizing sources within specific scenes relative to the microphone position. Some [47] use techniques like regression and classification, similar to those found in geolocation, while others work on applications like robotic navigation [8, 9] and audio-visual pose estimation [13]. While the structure of this problem is very similar to geolocation, the two tasks require very different signals.

There has been some prior work in geolocating speech, either as a proxy task for identifying accents and dialects [20, 43, 59], or to improve speech recognition (ASR) [3, 69]. Foley et al. [24] geolocate radio station broadcasts from around the world, but view locations solely as soft labels for language and focus on its benefit to few-shot language identification.

Geolocation Benchmarks. Standardized benchmarks have been central to progress in image geolocation, from early datasets like Im2GPS3K [31] to larger benchmarks such as Google World Streets 15K [16] and YFCC26K [45, 57]. In contrast, audio geolocation has relied on smaller datasets built for specific applications [14, 25, 26, 40, 48]. Datasets for soundscape mapping, such as SoundingEarth [32], GeoSound [38], and CVS [51] can also serve as testbeds for audio geolocation. Related benchmarks exist for aerial scene recognition [34] and voice retrieval [11, 12, 44]. While these benchmarks primarily feature urban sounds, our experiments shift attention to the natural domain, investigating the potential of wildlife sounds as geolocation signals.

3 Audio Geolocation: Problem Setup

The task of audio geolocation is defined as follows: given an audio recording x , the goal is to predict the coordinates $y = (\text{latitude}, \text{longitude})$ of the location where x was recorded. We evaluate the geolocation error by computing the Haversine distance between the predicted and true coordinates. Given a dataset $\mathcal{D} = \{(x_i, y_i)\}_{i=1}^N$ of audio recordings x_i and ground truth locations y_i , we measure the performance of a method using the median geolocation error across \mathcal{D} . Following standard practice in image geolocation [29, 60, 63], we also report “Percentage at Threshold,” where a prediction is considered correct if the geolocation error is within a specific threshold. We use thresholds of 25 km, 200 km, 750 km, and 2,500 km, corresponding to city, regional, country, and continental scales. Refer to Fig. 2 and supplementary Fig. A1 for illustrations of these scales.

iNatSounds Dataset. In this work, we conduct experiments using iNatSounds [7], a dataset of 230K audio recordings, with an average duration of 20s. Each recording is annotated with a species, recording date, and geographic location. The training split includes audio from over 5,500 species and spans diverse regions across the Americas, Africa, Europe, Asia, and Australia. However, the distribution is imbalanced, with a bias toward major population centers. See supplementary Fig. A4 for the geographic distribution of iNatSounds and Fig. 2 for some examples from around the world.

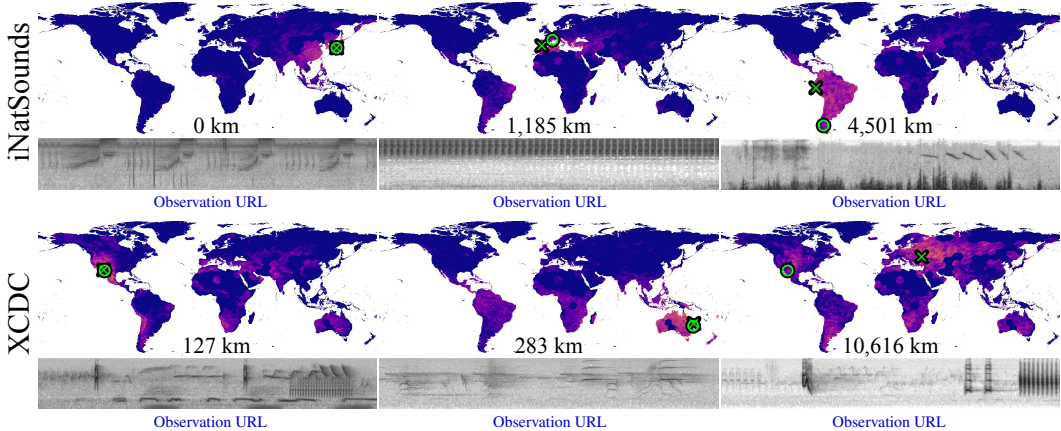


Figure 2: **Geolocation Predictions.** Sample predictions of our method on iNatSounds [7] and XCDC. Heatmap shows the unnormalized likelihood of each location. Green crosses denote the final prediction (argmax) and green circles denote true location. Geolocation error reported below each heatmap. URLs to the original observations provided below each spectrogram. Harshness of the region threshold (200km) can be better appreciated through the bottom left and center exemplars. Additional visualizations in supplemental Fig. A2, A3.

Sampling for Improved Geolocation. Short recordings often capture only a limited subset of species, which may constrain geolocation accuracy. To test whether models benefit from increased species diversity, we explore two strategies in Sec. 5.3: (1) using longer, species-rich recordings collected during the dawn chorus, and (2) aggregating multiple short recordings from the same spatiotemporal neighborhood.

4 Methods and Baselines

Preliminaries. Let $\mathbf{x} \in \mathcal{X}$ be an audio recording and \mathbf{y} be a location coordinate (lat, lon) from the geo-tagged dataset $\mathcal{D} = \{(\mathbf{x}_i, \mathbf{y}_i)\}_{i=1}^N$. Our goal is to train a model $g : \mathcal{X} \rightarrow \mathcal{L}$ where \mathcal{L} is the space of all possible locations. We decompose this model as $g = h_\phi \circ f_\theta$, where $f_\theta : \mathcal{X} \rightarrow \mathbb{R}^d$, is an audio encoder with parameters θ , and $h_\phi : \mathbb{R}^d \rightarrow \mathcal{L}$ is a decoder with parameters ϕ responsible for geolocating an audio feature. The location can be encoded in different ways, and the definition of \mathcal{L} changes accordingly. It can be simply (lat, lon) (for regression), a geographic bin label (for classification), or a learned embedding (for retrieval). Although the location encoding does not need to be reversible, each prediction in \mathcal{L} should be mappable to a corresponding (lat, lon) for evaluation.

Audio Encoder. We adopt a vision-inspired approach to acoustic analysis by converting audio to a spectrogram “image” and extracting features with computer vision backbones. Model architecture and pre-training details are described in Sec. 5 and spectrogram settings in supplemental Sec. A.5.

Regression for Geolocation. An intuitive approach is to directly regress latitude and longitude from $f_\theta(\mathbf{x})$. Here, h_ϕ is a linear layer with 2 outputs and the entire model is trained using either Euclidean distance or the differentiable Haversine distance as the loss. While the former offers simplicity, the latter is more accurate as we are computing distances on a sphere instead of a plane.

Classification for Geolocation. We can formulate geolocation as classification over a set of location bins. If the world is divided into bins, then the model can be trained using cross-entropy to predict the bin that contains the recording location. At test time, h_ϕ predicts a probability distribution over the bins and we use the center of the most probable bin as the predicted (lat, lon) coordinate.

Retrieval for Geolocation. We can pose the problem of geolocation as retrieval, where h_ϕ is responsible for computing the similarity of $f_\theta(\mathbf{x})$ (query) with a predefined collection of embeddings (keys). Recent prior work [60] has explored location encoders $l_\psi : \mathbb{R}^2 \rightarrow \mathbb{R}^d$, that learn dense representations for two-dimensional (lat, lon) values. We train h_ϕ to project audio features into the same embedding space as a location encoder. Retrieval can then be done at test time by comparing the predicted embedding $g(\mathbf{x}) \in \mathcal{L}$ against a gallery of precomputed location embeddings, and returning

the coordinates of the most similar location embedding. We use the training set itself to construct our gallery, so the predicted coordinates can be expressed as $\hat{\mathbf{y}} = \arg \max_{\mathbf{y}_j \in \mathcal{D}^{Tr}} g(\mathbf{x})^\top l_\psi(\mathbf{y}_j)$.

Species Oracles. We next explore methods specifically tailored for geolocating *natural* audio. We hypothesize that presence and absence of species is a strong signal for geolocation. One immediate challenge for testing this hypothesis is the unrealistic expectation of capturing sounds from all species in a location. In theory, if a recordist were to continuously capture audio at a location over an entire year, we might expect to record most species that occur there. With this complete “checklist” of species, how accurately can we predict recording location?

While year-long audio files are impractical, we can simulate these comprehensive checklists using precomputed species geographic range maps. For a given location on Earth, we determine which species’ ranges contain that location and construct a checklist of species that are present or absent. Although expert-verified range maps are not available for all species, recent advancements [17, 30] have enabled joint prediction of range maps for tens of thousands of species. We leverage one such model (SINR [17]), to construct range maps for all species in the iNatSounds dataset. Finally, we learn h_ϕ to perform retrieval style geolocation using these checklists instead of audio features. Note that checklist construction assumes oracle access to the true location. These experiments do not reflect a realistic audio geolocation setting, but instead serve as upper bounds for species-based approaches.

AG-CLIP. Our method, AudioGeo-CLIP, builds on top of GeoCLIP [60] and includes an auxiliary task of predicting SINR [17] checklists from audio. Concretely, we add a checklist decoder on top of f_θ , and an additional BCE loss with the species checklists. While a particular recording will likely capture only a small fraction of species whose ranges overlap the recording location, predicting the species checklist can encourage the encoder to attend not only to foreground vocalizations but also to background ambient sounds, learning to associate them with species likely to be encountered in that habitat. See supplemental Fig. A6 for a schematic.

Handling Variable Length. For a recording \mathbf{x} , we construct a collection of 3s “clips” using a sliding window. Each clip is geolocated independently and then the average of all clip-predictions is used as the final prediction for that recording. We experiment with alternate poolings in Sec. 5.2.

5 Experiments

Implementation Details. In the following experiments, f_θ is a trainable MobileNet-V3 [33] model pretrained for species classification on the iNatSounds dataset. These models expect spectrograms that have been resized to 224x224x3. For AG-CLIP, h_ϕ is composed of two 2-layer MLPs, each with hidden dimensions of 128, responsible for projecting features to GeoCLIP embeddings and SINR checklists, respectively. In Sec. 5.2, we further explore the impact of different network architectures and pretraining strategies for both audio and location encodings. All models are trained using SGD with nesterov acceleration. We use the validation set of iNatSounds to sweep learning rates and other hyperparameters. See supplemental Sec. A.5 for detailed model configurations.

5.1 Performance on iNatSounds

We present the performance of geolocation methods on the iNatSounds test set in Table 1.

Naive Baseline. We start with a naive baseline that samples a random location from the training distribution for each test recording. This baseline yields a regional accuracy of just 1.1%, suggesting that the dataset is sufficiently diverse and not dominated by a few geographic hotspots.

Species Oracles. To contextualize subsequent results, we first present upper-bound performance using species checklists constructed with oracle access to the true location. We binarize SINR [17] model outputs using a threshold of 0.1 to create binary vectors, or “checklists”, indicating species presence and absence at each location. We then train a linear model to serve as h_ϕ , predicting GeoCLIP embeddings and geolocating via retrieval. Our results indicate that with a *full checklist*, almost perfect region level performance is possible, confirming our hypothesis that species information serves as a strong geolocation signal. We simulate imperfect recall by randomly omitting a subset of species from the checklist. With 50% corruption, regional accuracy remains relatively high at 83.3%. If only 10 randomly selected species are retained, region performance drops to 37.6%. These partial checklists better reflect realistic scenarios with noisy or incomplete species identification.

Table 1: **Geolocation on iNatSounds.** Experiments on the iNatSounds test set. The naive random predictor and species oracles contextualize performance. We train our models to geolocate using regression, classification, explicit sampling from range maps and retrieval. Geolocation performance is evaluated by median error (km) and accuracies (%) at different distance thresholds. We report mean \pm std from 3 runs. \dagger : Off the shelf models.

Experiment		↓ Median Error (km)	↑ City 25km	Region 200km	Country 750km	Continent 2500km
Naive	Rnd Train Loc	7475 ± 32	00.1 ± 0.0	01.1 ± 0.0	06.6 ± 0.1	22.8 ± 0.3
Species Oracles	Full checklist	15 ± 00	64.0 ± 0.4	97.8 ± 0.0	99.9 ± 0.0	$100. \pm 0.0$
	50% Corrupted	54 ± 00	32.8 ± 0.0	83.3 ± 0.1	98.8 ± 0.0	$100. \pm 0.0$
	Keep random 10	325 ± 02	10.0 ± 0.1	37.6 ± 0.2	76.6 ± 0.2	98.3 ± 0.0
Regress	Euclidean	1884 ± 05	00.1 ± 0.0	02.9 ± 0.0	23.4 ± 0.2	57.9 ± 0.1
	Haversine	1602 ± 13	00.1 ± 0.0	04.2 ± 0.2	27.7 ± 0.3	61.8 ± 0.2
Classify	Res-0 ($430 \times 10^4 \text{ km}^2$)	1323 ± 09	00.0 ± 0.0	01.2 ± 0.0	22.6 ± 0.0	68.7 ± 0.2
	Res-2 ($8.6 \times 10^4 \text{ km}^2$)	1326 ± 12	00.3 ± 0.0	16.3 ± 0.2	36.5 ± 0.4	64.1 ± 0.2
	Hierarchical (0→1→2)	1117 ± 06	00.3 ± 0.0	16.6 ± 0.2	40.0 ± 0.1	68.7 ± 0.2
Species Ranges	Annotated Species	1263 ± 01	00.3 ± 0.0	10.8 ± 0.1	35.7 ± 0.1	72.3 ± 0.1
	Predicted Sp (Top 1)	1664 ± 03	00.2 ± 0.0	08.2 ± 0.1	28.7 ± 0.0	62.5 ± 0.1
	Predicted Sp (All)	1113 ± 02	00.3 ± 0.0	09.3 ± 0.1	37.7 ± 0.1	72.7 ± 0.1
Retrieve	GeoCLAP [37] [†]	6856 ± 00	00.2 ± 0.0	01.3 ± 0.0	07.0 ± 0.0	24.9 ± 0.0
	Taxabind [53] [†]	4944 ± 00	00.4 ± 0.0	02.2 ± 0.0	11.9 ± 0.0	35.3 ± 0.0
	AG-CLIP (ours)	1082 ± 11	06.4 ± 0.1	17.2 ± 0.1	41.0 ± 0.3	71.2 ± 0.2

Regress. Regression methods tend to do the worst overall, with region level performances of 2.9% and 4.2% for Euclidean and Haversine, respectively. Haversine distance more accurately captures geolocation error, which is the likely cause of its better performance as a loss function.

Classify. For classification, we use the H3 library [5] to divide the world into a hexagonal grid. h_ϕ is implemented as an N-way classifier where N is the number of hexagons in the grid. We experiment with two grid resolutions, defined by the area covered by each cell. More details and visualization of these grids are presented in supplemental Sec. A.3. Lower resolution (bigger cells) leads to better continental performance while higher resolution leads to better regional and country level performance. A hierarchical approach gets the best of both, performing similar to low resolution for continent (68.7% vs 68.7%) and better than high resolution for country (40.0% vs 36.5%).

Species Ranges. We next evaluate performance when explicit species information is available. Each iNatSounds recording includes a species annotation. By sampling the species’ SINR [17] likelihood distribution over a geographic grid, we can geolocate the recording. Note that SINR is trained on a much larger corpus of species occurrence data, which may offer an advantage over other methods. Using the annotated species, we see a region accuracy of 10.8% and a continent accuracy of 72.3%. However, the availability of ground-truth target species annotations at test time is unrealistic; instead, we can train a classifier to predict the target species from the audio [7]. Using the SINR distribution of the top-1 predicted target species drops the region and continent performance to 8.2% and 62.5% respectively. Rather than using a single predicted species for each recording, we can use the per-species scores given by our species classifier to weigh and combine SINR likelihood maps for all species. This weighted combination of species likelihood maps is slightly better than even the *annotated* target species (country 37.7% vs 35.7%, continent 72.7% vs 72.3%), which may be explained by the ability of these classifiers to capture background species to some extent [7].

Retrieve. For retrieval, we explore methods that jointly learn audio and location encoders. GeoCLAP [37] and Taxabind [53] are soundscape mapping methods that have their own audio and location encoders, which we use off-the-shelf without any additional training. GeoCLAP performs poorly, likely due to domain shift, as it was trained on urban sounds from SoundingEarth [32]. On the other hand, Taxabind, which was trained on a different subset of iNaturalist [35], achieves better results with a country level accuracy of 11.9%. However, it still underperforms compared to our models, likely because our models benefit from explicitly paired audio and location data, unlike the implicit pairing available through images for Taxabind. Our method, AG-CLIP, achieves the best performance overall, with region and country level performances of 17.2% and 41.0%, respectively.

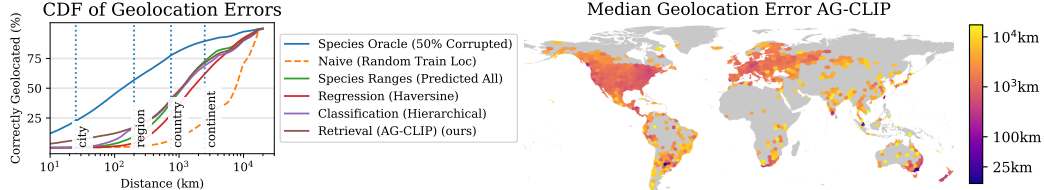


Figure 3: **Geolocation Error Trends.** Left: Cumulative distribution of geolocation errors for AG-CLIP and baseline models. Table 1 accuracy metrics correspond to points on these curves. Right: Median of AG-CLIP geolocation errors binned by H3 [5] hexagonal grid cells, capturing spatial variation in performance.

Model	Pre	FT	Reg.	Cont.	Experiment	City	Reg.	Cont.	Experiment	Reg.	Cont.
Wav2CLIP [65]	VGG [10]	X	03.8	30.3	SatCLIP [39]	1.4	14.7	63.2	Average	17.2	71.2
CLAP [23]	LAION [67]	X	05.1	34.6	SINR [17]	2.2	17.1	68.6	Max Pool	16.5	68.6
MobV3 [33]	ImgNet [21]	✓	14.4	64.9	GeoCLIP [60]	6.4	17.0	68.5	Cluster	15.5	67.9
MobV3 [33]	iNat [7]	✓	17.2	71.2	" + checklist	6.4	17.2	71.2	Transformer	16.8	71.5

(a) Audio Encoders

(b) Location Encoders

(c) Variable Length

Table 2: **Ablations.** Importance and alternative choices of different components of AG-CLIP. We include Region (Reg. 200km) and Continent (Cont. 2500km) performance on iNatSounds test set.

Performance at Different Distance Thresholds. Fig. 3 (left) shows CDF curves for various methods, plotting the fraction of test recordings (y-axis) correctly geolocated within a given distance (x-axis). These curves reveal how models perform across geospatial scales. Predictions based on species checklists, even with 50% corruption, is best across scales. Among audio geolocation methods, retrieval based AG-CLIP does best at finer scales like the city and region. Hierarchical classification shows a jump in performance around the region level and is close to AG-CLIP for coarser scales. This may be due to the finest grid cells being similar in size to a region, limiting the model’s ability to predict at finer resolutions. Explicit species identification with range analysis is relatively poor for finer scales, but overtakes AG-CLIP around the 1500 km mark.

Spatial Variation. Fig. 3 (right) shows how geolocation performance of AG-CLIP varies spatially. We associate each test recording with a resolution 2 hexagon from H3 [5] and compute the median error per hexagon. Darker (bluer) regions indicate better geolocation. The model performs better in regions with more training data, like the US and Europe. Interestingly, certain areas such as Central America, South Africa, Taiwan, Eastern Australia, and New Zealand show particularly good performance, possibly hinting at the presence of distinctive soundscapes in these regions.

5.2 Ablations

We ablate the audio encoders, location encoders, and temporal aggregation strategies in Table 2. Off-the-shelf audio encoders like Wav2CLIP [65] and CLAP [23] perform much worse than pretraining on iNatSounds (Table 2a). Starting with ImageNet pretrained weights instead of iNatSounds also reduces performance, with around 7% and 3% drops at the continent and region level, respectively.

Next, we ablate the location encoder in Table 2b. With SatCLIP [39], we observe consistently worse performance than SINR [17] or GeoCLIP [60]. SINR is comparable to GeoCLIP at the region and continent levels, but tapers off at the city level. Better performance of GeoCLIP may be because of its alignment with ground-level imagery, unlike SatCLIP (satellite images) or SINR (species observations). The auxiliary checklist loss introduced in AG-CLIP improves performance by 2.7% at the continent level, though the gains diminish at finer scales.

Finally, we explore alternate pooling methods to handle variable length audio in Table 2c. Our default is a simple average. We see a drop in performance if max-pooling is used instead. We could also first cluster the embeddings via K Means ($k=5$) and then use the centroid of the largest cluster as the aggregate. While better than max-pooling, this is still worse than averaging. We also try training a transformer model to pool frozen embeddings (see supplemental Sec. A.6 for more details). The transformer performs well at the continent level, but we prefer averaging because of its simplicity and lack of additional training.

Table 3: **Species-Rich Audio with XCDC.** Left: Models trained on iNatSounds training set and evaluated on XCDC. We report mean of 3 runs. Right: Geolocation with species ranges for randomly sampled subsets of ground truth species. We plot mean, std and range (min-max) over 100 runs.

Experiment	Error	City	Region	Cou.	Cont.
Species Ranges (True)	449	00.5	25.8	68.8	99.0
Species Ranges (Predicted)	1097	00.1	02.5	27.6	80.0
Classification (Hierarchical)	1116	00.0	05.3	31.7	69.7
AG-CLIP (ours)	1112	00.2	04.3	26.3	71.9

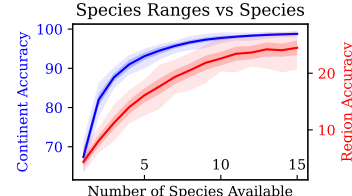
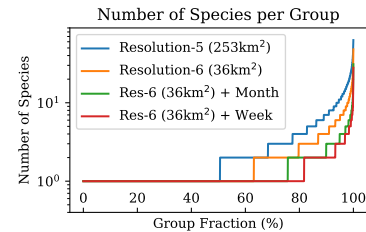


Table 4: **Spatiotemporal Aggregation.** Left: AG-CLIP geolocation can be improved by grouping recordings from the same neighborhood, over a year, month or week. Right: Distributions of unique species per collection.

Experiment	Error	City	Region	Cou.	Cont.
No Grouping	1082	06.4	17.2	41.0	71.2
Resolution-5 (253km^2)	520	13.2	30.4	62.1	88.2
Resolution-6 (36 km^2)	651	10.8	25.9	55.6	84.0
Res-6 (36 km^2) + Month	802	08.5	21.2	48.2	78.3
Res-6 (36 km^2) + Week	890	07.9	19.9	45.8	76.5



5.3 Geolocation with Species-Rich and Spatiotemporally Aggregated Recordings

Our species oracle experiments (Table 1) demonstrate that geolocation accuracy increases with the number of known species present at the recording location. However, short recordings often capture only a few species, limiting this important signal. To evaluate whether increased species diversity improves geolocation, we explore two strategies: (1) using long, species-rich recordings from the dawn chorus and (2) aggregating short recordings from the same spatiotemporal neighborhood.

Species-Rich Audio. We construct a dataset of species-rich audio by sampling dawn chorus recordings from Xeno-Canto [68], a global archive of natural sound recordings. The dawn chorus is a period of intense, multi-species vocal activity that occurs near sunrise, particularly during the breeding season [28, 62]. To isolate these species-rich recordings, we select audio that (1) was recorded during the spring dawn chorus, (2) is at least 3 minutes in duration, and (3) contains annotations for at least 10 distinct species. This filtering yields 576 recordings with associated geographic coordinates and species labels. We refer to this dataset as the Xeno-Canto Dawn Chorus (XCDC), a new benchmark for evaluating geolocation from species-rich soundscapes.

Our results are shown in Table 3. We reconfirm the value of species information: geolocation accuracy increases as more ground truth species are provided (Table 3, right), with full species knowledge yielding a region-level accuracy of 25.8% (Table 3, top row). However, model-based approaches that rely on predicted species ranges, hierarchical classification, or retrieval achieve substantially lower performance ($\leq 5.3\%$), roughly equivalent to knowing only a single species. This suggests that current models struggle to exploit the multi-species signals present in these complex soundscapes. One likely explanation is a distribution shift: most iNatSounds recordings contain far fewer species, and models trained on such data may not generalize well to species-rich audio.

Spatiotemporal Aggregation. We group iNatSounds test recordings by location and time to simulate spatiotemporal aggregation. Spatial grouping is performed using H3 [5] hexagons at resolutions 5 and 6, while temporal grouping spans the full year, individual months (12), or individual weeks (52). To geolocate a group, we first apply our model independently to each recording, then average the predicted location distributions across the group. The aggregated prediction is assigned to all recordings in the group, allowing direct comparison with recording-level results from Table 1.

Table 4 reports AG-CLIP performance under different spatiotemporal aggregation strategies. Aggregating recordings across the full year within 253 km^2 neighborhoods improves region-level accuracy from 17.2% (no grouping) to 30.4%. Reducing the spatial extent to 36 km^2 yields a more modest improvement to 25.9%. When aggregation is limited to a single month or week, performance drops to 21.2% and 19.9%, respectively. This drop reflects the limited species diversity under finer temporal

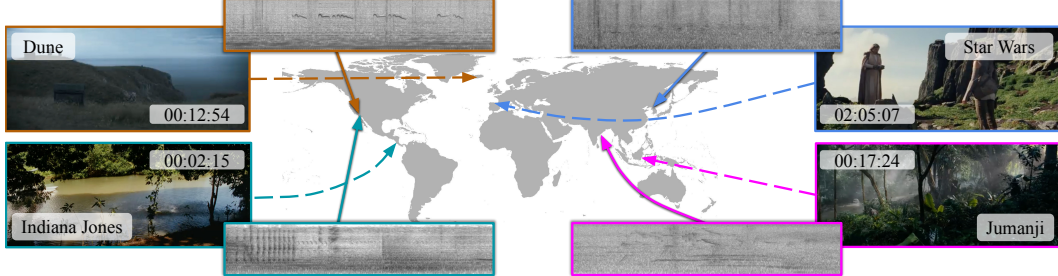


Figure 4: **Multimodal Geo-Forensics with Movie Clips.** Geolocation predictions for audio and video frames from scenes in four movies. Arrows on the map indicate the predicted locations for each modality. Discrepancies between modalities reveal potential artifacts introduced during post-production.

resolutions: as shown in the right panel of Table 4, over 80% of groups in the weekly grouping contain only a single species. Still, the modest gains relative to the ungrouped baseline suggest that the model is able to leverage complementary species information spread across multiple recordings.

5.4 Multimodal Geo-Forensics

Live broadcasts of events, such as professional golf tournaments, often enhance their ambiance by inserting bird vocalizations. However, observers have noted cases where producers mistakenly included species not found at the event location [36]. Similar mismatches arise in film, where audio effects may not correspond to the geographic setting depicted on screen [18, 22]. These inconsistencies offer a unique opportunity for *multimodal geo-forensics*.

To explore this idea, we analyze scenes from four Hollywood films, with results shown in Fig. 4. We selected scenes that had been previously flagged by viewers for mismatches between visual setting and soundscape. In all cases, audio- and image-based geolocation produced divergent predictions, confirming the presence of modality inconsistencies. Jumanji showed the closest alignment between modalities at 4480 km, while Star Wars exhibited the largest divergence at 9092 km. These qualitative results highlight the potential of multimodal geo-forensics as a novel application domain, leveraging cross-modal cues to identify geographic inconsistencies. We view this as a promising direction for future work at the intersection of vision, sound, and place. See supplemental Sec. A.9 for more details.

6 Conclusion

Geolocating arbitrary audio is challenging, but recordings containing wildlife sounds offer promising signals. Wildlife sounds can be explicitly identified and linked to known species ranges, or implicitly leveraged by end-to-end models. Our species oracle experiments show that when at least 10 species are detected, geolocation within 200 km is possible 37% of the time (Table 1). However, in species-rich recordings from XCDC, our species classification models achieve only 2.5% region accuracy (Table 3), highlighting a gap in current multi-species detection capabilities. On shorter, focused recordings, species-range models perform better (9.3%), and end-to-end models achieve 17.2% region accuracy (Table 1). Aggregating predictions across recordings from spatiotemporal neighborhoods of size 36 km² further improves performance to 25.9% (Table 4).

Future work could improve species classification in complex soundscapes, develop architectures that better capture long-range acoustic context, and explore structured fusion across multiple recordings. Collecting training data with dense species sounds may help address distributional shifts relative to datasets like XCDC. Our multimodal geo-forensics case studies highlight opportunities for combining audio and visual signals to detect inconsistencies in media, opening new directions for datasets, methods, and applications with both scientific and societal relevance.

Finally, we note important limitations and societal impact. iNatSounds exhibits geographic bias towards Western countries, particularly in the Northern Hemisphere, which affects both training and evaluation. Audio geolocation also poses potential privacy risks if applied to online media without user consent. Conversely, these tools could support transparency and authenticity in public media by detecting manipulated or misattributed content.

References

- [1] Josh Achiam, Steven Adler, Sandhini Agarwal, Lama Ahmad, Ilge Akkaya, Florencia Leoni Aleman, Diogo Almeida, Janko Altenschmidt, Sam Altman, Shyamal Anadkat, et al. Gpt-4 technical report. *arXiv preprint arXiv:2303.08774*, 2023.
- [2] Luca Maria Aiello, Rossano Schifanella, Daniele Quercia, and Francesco Aletta. Chatty maps: constructing sound maps of urban areas from social media data. *Royal Society open science*, 3(3):150690, 2016.
- [3] Peter Bell, Catherine Lai, Clare Llewellyn, Alexandra Birch, and Mark Sinclair. A system for automatic broadcast news summarisation, geolocation and translation. In *INTERSPEECH 2015 16th Annual Conference of the International Speech Communication Association*, pages 730–731, 2015.
- [4] Gabriele Berton, Carlo Masone, and Barbara Caputo. Rethinking visual geo-localization for large-scale applications. In *Proceedings of the IEEE/CVF Conference on Computer Vision and Pattern Recognition*, pages 4878–4888, 2022.
- [5] Isaac Brodsky. H3: Hexagonal hierarchical geospatial indexing system. *Uber Open Source*. Retrieved, 2018.
- [6] Deng Cai, Yan Wang, Lemao Liu, and Shuming Shi. Recent advances in retrieval-augmented text generation. In *Proceedings of the 45th international ACM SIGIR conference on research and development in information retrieval*, pages 3417–3419, 2022.
- [7] Mustafa Chasmai, Alexander Shepard, Subhransu Maji, and Grant Van Horn. The inaturalist sounds dataset. In *Proceedings of the 38th International Conference on Neural Information Processing Systems Datasets and Benchmarks Track*, 2024.
- [8] Changan Chen, Unnat Jain, Carl Schissler, Sebastia Vicenc Amengual Gari, Ziad Al-Halah, Vamsi Krishna Ithapu, Philip Robinson, and Kristen Grauman. Soundspaces: Audio-visual navigation in 3d environments. In *Computer Vision–ECCV 2020: 16th European Conference, Glasgow, UK, August 23–28, 2020, Proceedings, Part VI 16*, pages 17–36. Springer, 2020.
- [9] Changan Chen, Ziad Al-Halah, and Kristen Grauman. Semantic audio-visual navigation. In *Proceedings of the IEEE/CVF Conference on Computer Vision and Pattern Recognition*, pages 15516–15525, 2021.
- [10] Honglie Chen, Weidi Xie, Andrea Vedaldi, and Andrew Zisserman. Vggsound: A large-scale audio-visual dataset. In *ICASSP 2020-2020 IEEE International Conference on Acoustics, Speech and Signal Processing (ICASSP)*, pages 721–725. IEEE, 2020.
- [11] Yaxiong Chen and Xiaoqiang Lu. A deep hashing technique for remote sensing image-sound retrieval. *Remote Sensing*, 12(1):84, 2019.
- [12] Yaxiong Chen, Xiaoqiang Lu, and Shuai Wang. Deep cross-modal image-voice retrieval in remote sensing. *IEEE Transactions on Geoscience and Remote Sensing*, 58(10):7049–7061, 2020.
- [13] Ziyang Chen, Shengyi Qian, and Andrew Owens. Sound localization from motion: Jointly learning sound direction and camera rotation. In *Proceedings of the IEEE/CVF International Conference on Computer Vision*, pages 7897–7908, 2023.
- [14] Jaeyoung Choi, Gerald Friedland, et al. *Multimodal location estimation of videos and images*. Springer, 2015.
- [15] Ming-An Chung, Hung-Chi Chou, and Chia-Wei Lin. Sound localization based on acoustic source using multiple microphone array in an indoor environment. *Electronics*, 11(6):890, 2022.
- [16] Brandon Clark, Alec Kerrigan, Parth Parag Kulkarni, Vicente Vivanco Cepeda, and Mubarak Shah. Where we are and what we’re looking at: Query based worldwide image geo-localization using hierarchies and scenes. In *Proceedings of the IEEE/CVF Conference on Computer Vision and Pattern Recognition*, pages 23182–23190, 2023.
- [17] Elijah Cole, Grant Van Horn, Christian Lange, Alexander Shepard, Patrick Leary, Pietro Perona, Scott Loarie, and Oisin Mac Aodha. Spatial implicit neural representations for global-scale species mapping. In *International Conference on Machine Learning*, pages 6320–6342. PMLR, 2023.
- [18] Counterfeit Birds: The Mishaps of Birding at the Movies. <https://www.ornitheology.com/post/birdwatching-at-the-movies>, 2025. Accessed on May 1, 2025.

[19] Xudong Dang, Qi Cheng, and Hongyan Zhu. Indoor multiple sound source localization via multi-dimensional assignment data association. *IEEE/ACM Transactions on Audio, Speech, and Language Processing*, 27(12):1944–1956, 2019.

[20] Najim Dehak, Patrick J Kenny, Réda Dehak, Pierre Dumouchel, and Pierre Ouellet. Front-end factor analysis for speaker verification. *IEEE Transactions on Audio, Speech, and Language Processing*, 19(4):788–798, 2010.

[21] Jia Deng, Wei Dong, Richard Socher, Li-Jia Li, Kai Li, and Li Fei-Fei. Imagenet: A large-scale hierarchical image database. In *2009 IEEE conference on computer vision and pattern recognition*, pages 248–255. Ieee, 2009.

[22] DUNE - Who knows the bird call from Caladan? https://www.reddit.com/r/Norway/comments/rqv170/dune_who_knows_the_bird_call_from_caladan/?rdt=39315, 2025. Accessed on May 1, 2025.

[23] Benjamin Elizalde, Soham Deshmukh, Mahmoud Al Ismail, and Huaming Wang. Clap: learning audio concepts from natural language supervision. In *ICASSP 2023-2023 IEEE International Conference on Acoustics, Speech and Signal Processing (ICASSP)*, pages 1–5. IEEE, 2023.

[24] Patrick Foley, Matthew Wiesner, Bismarck Odoom, Leibny Paola Garcia Perera, Kenton Murray, and Philipp Koehn. Where are you from? geolocating speech and applications to language identification. In *Proceedings of the 2024 Conference of the North American Chapter of the Association for Computational Linguistics: Human Language Technologies (Volume 1: Long Papers)*, pages 5114–5126, 2024.

[25] Gerald Friedland, Oriol Vinyals, and Trevor Darrell. Multimodal location estimation. In *Proceedings of the 18th ACM international conference on Multimedia*, pages 1245–1252, 2010.

[26] Gerald Friedland, Jaeyoung Choi, Howard Lei, and Adam Janin. Multimodal location estimation on flickr videos. In *Proceedings of the 3rd ACM SIGMM international workshop on Social media*, pages 23–28, 2011.

[27] GeoGuessr. Geoguessr - let's explore the world!, 2013. URL <https://www.geoguessr.com/>. Accessed on May 1, 2025.

[28] Diego Gil and Diego Llusia. The bird dawn chorus revisited. *Coding strategies in vertebrate acoustic communication*, pages 45–90, 2020.

[29] Lukas Haas, Michal Skreta, Silas Alberti, and Chelsea Finn. Pigeon: Predicting image geolocations. In *Proceedings of the IEEE/CVF Conference on Computer Vision and Pattern Recognition*, pages 12893–12902, 2024.

[30] Max Hamilton, Christian Lange, Elijah Cole, Alexander Shepard, Samuel Heinrich, Oisin Mac Aodha, Grant Van Horn, and Subhransu Maji. Combining observational data and language for species range estimation. In *The Thirty-eighth Annual Conference on Neural Information Processing Systems*, 2024.

[31] James Hays and Alexei A Efros. Im2gps: estimating geographic information from a single image. In *2008 ieee conference on computer vision and pattern recognition*, pages 1–8. IEEE, 2008.

[32] Konrad Heidler, Lichao Mou, Di Hu, Pu Jin, Guangyao Li, Chuang Gan, Ji-Rong Wen, and Xiao Xiang Zhu. Self-supervised audiovisual representation learning for remote sensing data. *International Journal of Applied Earth Observation and Geoinformation*, 116:103130, 2023.

[33] Andrew Howard, Mark Sandler, Grace Chu, Liang-Chieh Chen, Bo Chen, Mingxing Tan, Weijun Wang, Yukun Zhu, Ruoming Pang, Vijay Vasudevan, et al. Searching for mobilenetv3. In *Proceedings of the IEEE/CVF international conference on computer vision*, pages 1314–1324, 2019.

[34] Di Hu, Xuhong Li, Lichao Mou, Pu Jin, Dong Chen, Liping Jing, Xiaoxiang Zhu, and Dejing Dou. Cross-task transfer for geotagged audiovisual aerial scene recognition. In *Computer Vision–ECCV 2020: 16th European Conference, Glasgow, UK, August 23–28, 2020, Proceedings, Part XXIV 16*, pages 68–84. Springer, 2020.

[35] iNaturalist. <https://www.inaturalist.org>, 2025. Accessed on May 1, 2025.

[36] Is CBS Piping Fake Birds Into Its Masters Coverage? <https://slate.com/culture/2019/04/masters-cbs-coverage-birds-real-fake.html>, 2025. Accessed on May 1, 2025.

[37] Subash Khanal, Srikumar Sastry, Aayush Dhakal, and Nathan Jacobs. Learning tri-modal embeddings for zero-shot soundscape mapping. In *BMVC*, 2023.

[38] Subash Khanal, Eric Xing, SriKumar Sastry, Aayush Dhakal, Zhexiao Xiong, Adeel Ahmad, and Nathan Jacobs. Psm: Learning probabilistic embeddings for multi-scale zero-shot soundscape mapping. In *ACM Multimedia*, 2024.

[39] Konstantin Klemmer, Esther Rolf, Caleb Robinson, Lester Mackey, and Marc Rußwurm. Satclip: Global, general-purpose location embeddings with satellite imagery. *arXiv preprint arXiv:2311.17179*, 2023.

[40] A. Kumar, B. Elizalde, and B. Raj. Audio content based geotagging in multimedia. In *Proceedings of Interspeech 2017*, pages 1874–1878, 2017. doi: 10.21437/Interspeech.2017-40.

[41] Hangxin Liu, Zeyu Zhang, Yixin Zhu, and Song-Chun Zhu. Self-supervised incremental learning for sound source localization in complex indoor environment. In *2019 International Conference on Robotics and Automation (ICRA)*, pages 2599–2605, 2019. doi: 10.1109/ICRA.2019.8794231.

[42] Liu Liu and Hongdong Li. Lending orientation to neural networks for cross-view geo-localization. In *Proceedings of the IEEE/CVF conference on computer vision and pattern recognition*, pages 5624–5633, 2019.

[43] Georg Lohfink. The "sprekend nederland" project applied to accent location. Master's thesis, Utrecht University, 2017.

[44] Guo Mao, Yuan Yuan, and Lu Xiaoqiang. Deep cross-modal retrieval for remote sensing image and audio. In *2018 10th IAPR workshop on pattern recognition in remote sensing (PRRS)*, pages 1–7. IEEE, 2018.

[45] Eric Muller-Budack, Kader Pustu-Iren, and Ralph Ewerth. Geolocation estimation of photos using a hierarchical model and scene classification. In *Proceedings of the European conference on computer vision (ECCV)*, pages 563–579, 2018.

[46] Paul Pedersen. The mel scale. *Journal of Music Theory*, 9(2):295–308, 1965.

[47] Lauréline Perotin, Alexandre Défossez, Emmanuel Vincent, Romain Serizel, and Alexandre Guérin. Regression versus classification for neural network based audio source localization. In *2019 IEEE Workshop on Applications of Signal Processing to Audio and Acoustics (WASPAA)*, pages 343–347. IEEE, 2019.

[48] Florian B Pokorny, Moritz Fišer, Franz Graf, Peter B Marschik, and Björn W Schuller. Sound and the city: Current perspectives on acoustic geo-sensing in urban environment. *Acta Acustica united with Acustica*, 105(5):766–778, 2019.

[49] Shraman Pramanick, Ewa M Nowara, Joshua Gleason, Carlos D Castillo, and Rama Chellappa. Where in the world is this image? transformer-based geo-localization in the wild. In *European Conference on Computer Vision*, pages 196–215. Springer, 2022.

[50] Alec Radford, Jong Wook Kim, Chris Hallacy, Aditya Ramesh, Gabriel Goh, Sandhini Agarwal, Girish Sastry, Amanda Askell, Pamela Mishkin, Jack Clark, et al. Learning transferable visual models from natural language supervision. In *International conference on machine learning*, pages 8748–8763. PMLR, 2021.

[51] Tawfiq Salem, Menghua Zhai, Scott Workman, and Nathan Jacobs. A multimodal approach to mapping soundscapes. In *Proceedings of the IEEE Conference on Computer Vision and Pattern Recognition Workshops*, pages 2524–2527, 2018.

[52] Tawfiq Salem, Menghua Zhai, Scott Workman, and Nathan Jacobs. A multimodal approach to mapping soundscapes. In *IEEE International Geoscience and Remote Sensing Symposium (IGARSS)*, 2018. doi: 10.1109/IGARSS.2018.8517977.

[53] SriKumar Sastry, Subash Khanal, Aayush Dhakal, Adeel Ahmad, and Nathan Jacobs. Taxabind: A unified embedding space for ecological applications. In *Winter Conference on Applications of Computer Vision*. IEEE/CVF, 2025.

[54] Paul Hongsuck Seo, Tobias Weyand, Jack Sim, and Bohyung Han. Cplanet: Enhancing image geolocation by combinatorial partitioning of maps. In *Proceedings of the European Conference on Computer Vision (ECCV)*, pages 536–551, 2018.

[55] Yujiao Shi, Xin Yu, Dylan Campbell, and Hongdong Li. Where am i looking at? joint location and orientation estimation by cross-view matching. In *Proceedings of the IEEE/CVF Conference on Computer Vision and Pattern Recognition*, pages 4064–4072, 2020.

[56] Yingxiang Sun, Jiajia Chen, Chau Yuen, and Susanto Rahardja. Indoor sound source localization with probabilistic neural network. *IEEE Transactions on Industrial Electronics*, 65(8):6403–6413, 2017.

[57] Bart Thomee, David A Shamma, Gerald Friedland, Benjamin Elizalde, Karl Ni, Douglas Poland, Damian Borth, and Li-Jia Li. Yfcc100m: The new data in multimedia research. *Communications of the ACM*, 59(2):64–73, 2016.

[58] Hugo Touvron, Thibaut Lavril, Gautier Izacard, Xavier Martinet, Marie-Anne Lachaux, Timothée Lacroix, Baptiste Rozière, Naman Goyal, Eric Hambro, Faisal Azhar, et al. Llama: Open and efficient foundation language models. *arXiv preprint arXiv:2302.13971*, 2023.

[59] David A Van Leeuwen and Rosemary Orr. The "sprekend nederland" project and its application to accent location. *arXiv preprint arXiv:1602.02499*, 2016.

[60] Vicente Vivanco Cepeda, Gaurav Kumar Nayak, and Mubarak Shah. Geoclip: Clip-inspired alignment between locations and images for effective worldwide geo-localization. *Advances in Neural Information Processing Systems*, 36, 2024.

[61] Nam Vo, Nathan Jacobs, and James Hays. Revisiting im2gps in the deep learning era. In *Proceedings of the IEEE international conference on computer vision*, pages 2621–2630, 2017.

[62] Matthew James Weldy, Tom Denton, Abram B Fleishman, Jaclyn Tolchin, Matthew McKown, Robert S Spaan, Zachary J Ruff, Julianna MA Jenkins, Matthew G Betts, and Damon B Lesmeister. Audio tagging of avian dawn chorus recordings in california, oregon and washington. *Biodiversity Data Journal*, 12:e118315, 2024.

[63] Tobias Weyand, Ilya Kostrikov, and James Philbin. Planet-photo geolocation with convolutional neural networks. In *Computer Vision–ECCV 2016: 14th European Conference, Amsterdam, The Netherlands, October 11–14, 2016, Proceedings, Part VIII 14*, pages 37–55. Springer, 2016.

[64] Scott Workman, Richard Souvenir, and Nathan Jacobs. Wide-area image geolocalization with aerial reference imagery. In *Proceedings of the IEEE International Conference on Computer Vision*, pages 3961–3969, 2015.

[65] Ho-Hsiang Wu, Prem Seetharaman, Kundan Kumar, and Juan Pablo Bello. Wav2clip: Learning robust audio representations from clip. In *ICASSP 2022-2022 IEEE International Conference on Acoustics, Speech and Signal Processing (ICASSP)*, pages 4563–4567. IEEE, 2022.

[66] Yifan Wu, Roshan Ayyalasomayajula, Michael J Bianco, Dinesh Bharadvia, and Peter Gerstoft. Sslide: Sound source localization for indoors based on deep learning. In *ICASSP 2021-2021 IEEE International Conference on Acoustics, Speech and Signal Processing (ICASSP)*, pages 4680–4684. IEEE, 2021.

[67] Yusong Wu, Ke Chen, Tianyu Zhang, Yuchen Hui, Taylor Berg-Kirkpatrick, and Shlomo Dubnov. Large-scale contrastive language-audio pretraining with feature fusion and keyword-to-caption augmentation. In *ICASSP 2023-2023 IEEE International Conference on Acoustics, Speech and Signal Processing (ICASSP)*, pages 1–5. IEEE, 2023.

[68] Xeno-Canto. <https://xeno-canto.org>, 2025. Accessed on May 1, 2025.

[69] Xiaoqiang Xiao, Hong Chen, Mark Zylak, Daniela Sosa, Suma Desu, Mahesh Krishnamoorthy, Daben Liu, Matthias Paulik, and Yuchen Zhang. Geographic language models for automatic speech recognition. In *2018 IEEE International Conference on Acoustics, Speech and Signal Processing (ICASSP)*, pages 6124–6128. IEEE, 2018.

[70] Hongji Yang, Xiufan Lu, and Yingying Zhu. Cross-view geo-localization with layer-to-layer transformer. *Advances in Neural Information Processing Systems*, 34:29009–29020, 2021.

[71] Xiaomeng Zhang, Hao Sun, Shuopeng Wang, and Jing Xu. A new regional localization method for indoor sound source based on convolutional neural networks. *IEEE Access*, 6:72073–72082, 2018.

[72] Zhongliang Zhou, Jielu Zhang, Zihan Guan, Mengxuan Hu, Ni Lao, Lan Mu, Sheng Li, and Gengchen Mai. Img2loc: Revisiting image geolocalization using multi-modality foundation models and image-based retrieval-augmented generation. In *Proceedings of the 47th International ACM SIGIR Conference on Research and Development in Information Retrieval*, pages 2749–2754, 2024.

[73] Sijie Zhu, Taojinnan Yang, and Chen Chen. Vigor: Cross-view image geo-localization beyond one-to-one retrieval. In *Proceedings of the IEEE/CVF Conference on Computer Vision and Pattern Recognition*, pages 3640–3649, 2021.

[74] Sijie Zhu, Mubarak Shah, and Chen Chen. Transgeo: Transformer is all you need for cross-view image geo-localization. In *Proceedings of the IEEE/CVF Conference on Computer Vision and Pattern Recognition*, pages 1162–1171, 2022.

A Appendix

Benchmark (iNatSounds + XCDC): [cvl-umass/nat-sound2loc-benchmark](https://github.com/cvl-umass/nat-sound2loc-benchmark).

Codebase (model training and reproduction): [cvl-umass/nat-sound2loc-code](https://github.com/cvl-umass/nat-sound2loc-code).

We start with a visualization of the distance thresholds used by our evaluation metrics in Sec. A.1. We follow this with additional prediction visualizations in Sec. A.2. Next, we visualize the different ways to represent location for classification (Sec. A.3) and retrieval (Sec. A.4). We next describe additional implementation details left out in the main paper (see Sec. A.5). In particular, we elaborate on the methodology with a block diagram, describe the spectrogram creation process, and report tuned hyperparameters and other configurations. We also share additional details for GeoCLAP and TaxaBind as well as the transformer pooling ablation (Sec. A.6) in Table 2 (main paper). Next, in Sec. A.7, we report additional ablation on Location Galleries. Additional results and standard deviations for XCDC are reported and discussed in Sec. A.8. Next, we report additional details for geoforensics experiments (Sec. A.9) and present additional experiments on multimodal geolocation (Sec. A.10), species affinities (Sec. A.11) and multimodal retrieval (Sec. A.12). We conclude with a discussion on compute resources in Sec. A.13.

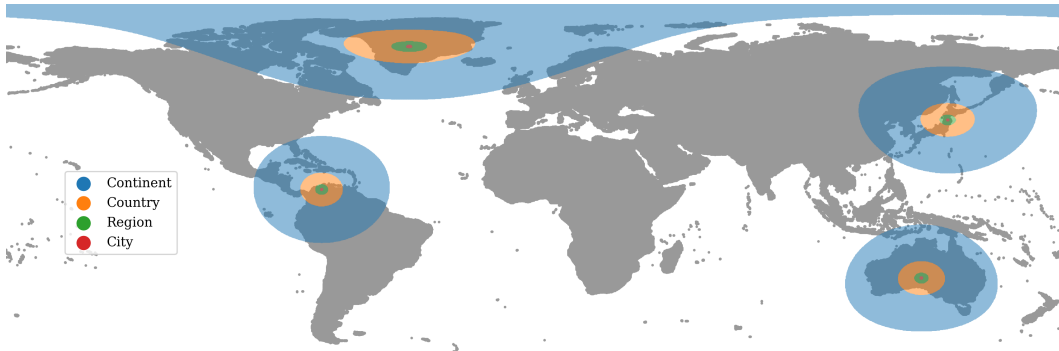


Figure A1: **Scales of Geolocation.** We plot all points within different thresholds used for calculating our geolocation metrics. These are not circles because we use haversine distance. We show these scales centered at a few different locations since the size changes at different points on earth.

A.1 Scales of Geolocation

For better understanding of the distance thresholds used in evaluation and an appreciation of the difficulty of this task, please see their visualization in Fig A1. A prediction is considered correct at a given level if it falls within the corresponding area centered on the ground-truth location. Note the great difference in scale between finer levels like the city (barely bigger than a dot) and coarser levels like the country and continent. While 200km for the region level may sound large, the small green areas in Fig A1 show how small it is compared to the size of the world. Even the continent threshold is actually harsher than it sounds, and covers only about the size of Australia.

A.2 More Prediction Visualizations

See additional prediction visualizations of AG-CLIP on iNatSounds and XCDC in Fig A2 and Fig A3 respectively. These are a mix of success and failure cases of the model.

A.3 Classification Grids.

We visualize the different resolution hexagonal grids we use for classification in Fig A4. We train the model to predict a hexagon from the list of all possible hexagons at a particular resolution. At test time, we use the center of the predicted hexagon as the geolocation prediction. As we go to finer resolutions, the ability of a classifier to pinpoint to finer scales increases. At the same time, the total number of hexagons also increases, which reduces classification performance.

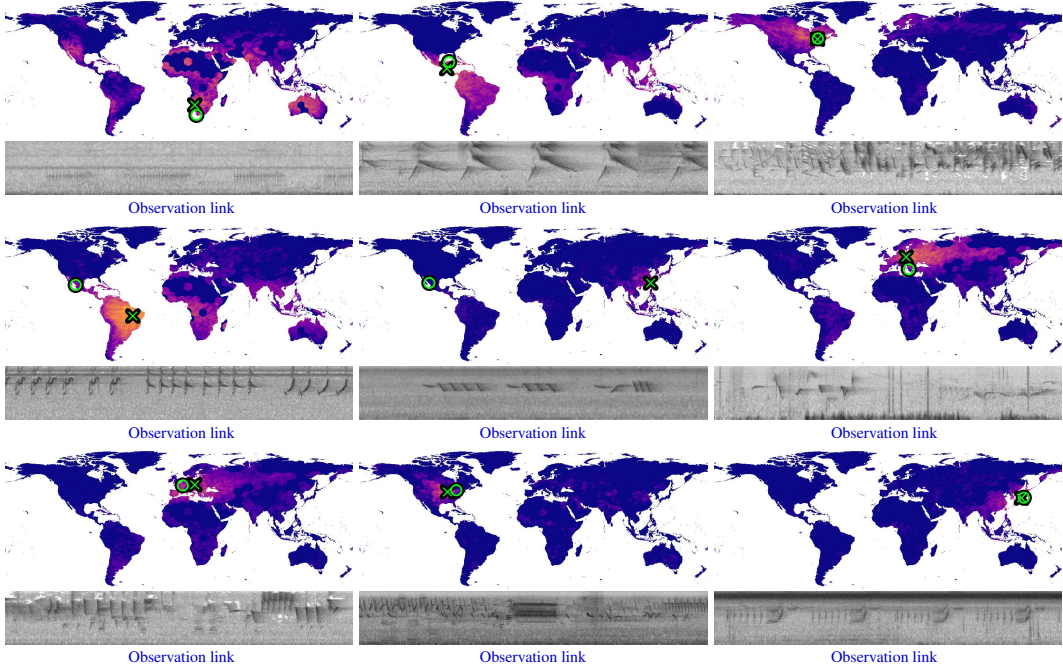


Figure A2: **Model Predictions on iNatSounds [7].** Heatmap shows the unnormalised likelihood of each location. Green crosses denote the final prediction (argmax) and green circles denote true location. Original observations linked below. Best viewed zoomed in.

We also show the distribution of iNatSounds training set on the same plots. The distribution is highly imbalanced, with North America and Europe having significantly higher number of recordings than other areas.

A.4 Retrieval Location Galleries.

Location retrieval approaches like ours require a gallery of candidate locations to retrieve from at test time. An advantage of this approach over image retrieval approaches is that candidate locations can be sampled readily (just 2 coordinates) and do not require a database at test time. However, construction of these location galleries can affect final performance. A gallery that is too sparse can lead to higher geolocation errors and a gallery that is too dense can require too much compute. See Fig A5 for visualization of different galleries.

A.5 Additional Implementation Details

Spectrogram Creation. We take a vision approach where 1D waveforms are converted to 2D spectrograms, which can be treated as images. Following previous work [7], we generate spectrograms using the Short-Time Fourier transform (STFT), with a window size of 512 and a stride length of 128. Linear spaced frequencies are converted to the mel-scale [46], mapping frequencies in the range [50Hz, 11.025kHz] to 128 logarithmically spaced mel bins, better aligning with human perception of pitch change. Each audio recording is split into a set of windows of 3 seconds each, strided by 1.5 seconds. Each window is treated as an independent image, repeated thrice and resized to get a $224 \times 224 \times 3$ RGB input.

Classification for Geolocation. We can formulate geolocation as classification over a set of location bins. If the world is divided into bins, then h_ϕ can be trained using cross-entropy to predict the bin that contains the recording location.

At test time, h_ϕ predicts a probability distribution over the bins and we use the center of the most likely bin as the predicted location. The bin resolution (large bin area vs small bin area) imposes constraints on the maximum achievable performance since even correctly classified (i.e., correctly binned) samples may be far from the bin center. This is likely the cause of the very poor regional

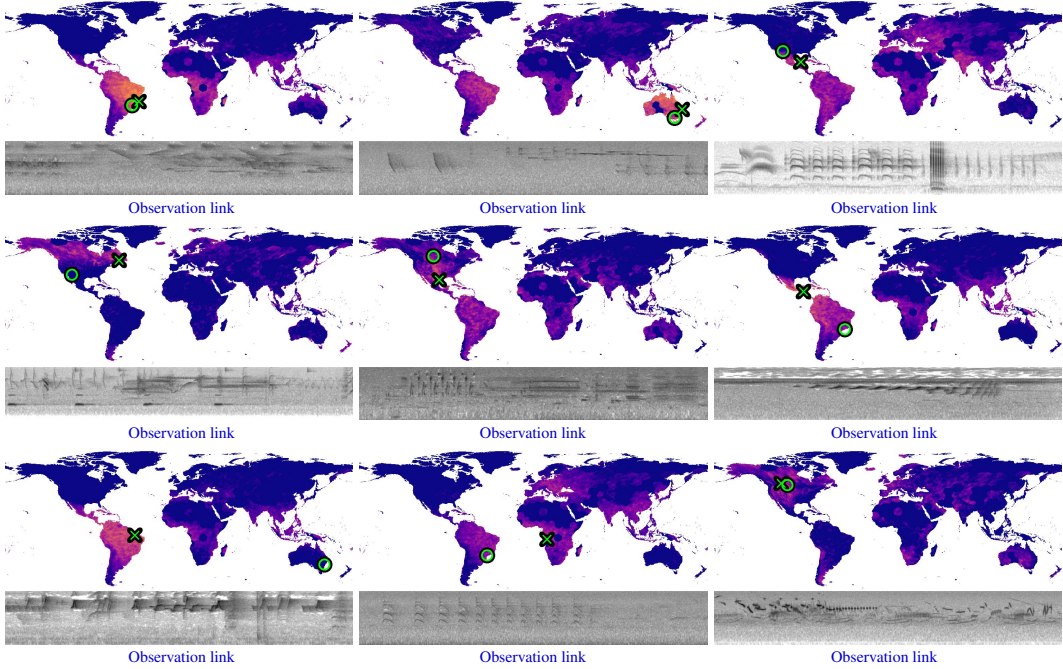


Figure A3: **Model Predictions on XCDC.** Heatmap shows the unnormalised likelihood of each location. Green crosses denote the final prediction (argmax) and green circles denote true location. Original observations linked below. Best viewed zoomed in.

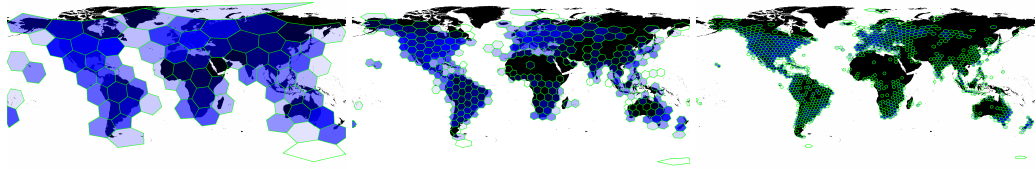


Figure A4: **Classification grids and iNatSounds Distribution.** Visualization of H3 [5] grid cells at different resolutions (0, 1 and 2 from left to right with average cell areas 436, 61 and $9 \times 10^4 \text{ km}^2$ respectively). In the hexagon itself, we show the actual distribution of the iNatSounds training set (higher opacity \rightarrow more data). We use log scale for better visualization.

performance with lowest resolution models in Table 1 (main paper). For higher resolution cells, the size of each cell is smaller, and thus, the error introduced by choosing the grid center is lower. However, higher resolution grids have more cells, or classes, which makes the classification itself somewhat harder.

We also experiment with a hierarchical approach to better handle this tradeoff. A low resolution model first predicts a large cell. Then a higher resolution model is used to predict a smaller cell within this large cell. This can be repeated for multiple levels of hierarchy. We start with resolution 0, followed by resolution 1 and finally 2. Note that this is done only at test time, so once the models at different resolution are trained, they can just be used directly for hierarchical classification.

Model Architecture and Hyperparameters. We show a block diagram of the AG-CLIP model architecture in Fig. A6. The pipeline has some differences at training and test times. While training, we sample windows uniformly at random from audio recordings, while at test time, we densely sample strided windows from the entire audio recording and aggregate to get recording level predictions.

In all experiments, we use the relatively light-weight MobileNet V3 [33] as our audio backbone to get a 1280 dimensional features from windows resized to 224×224 . We choose model dimension hyperparameters to get good performance while keeping model size comparable. Our checklist prediction head learns to predict the entire species checklist given by SINR. The projection layer

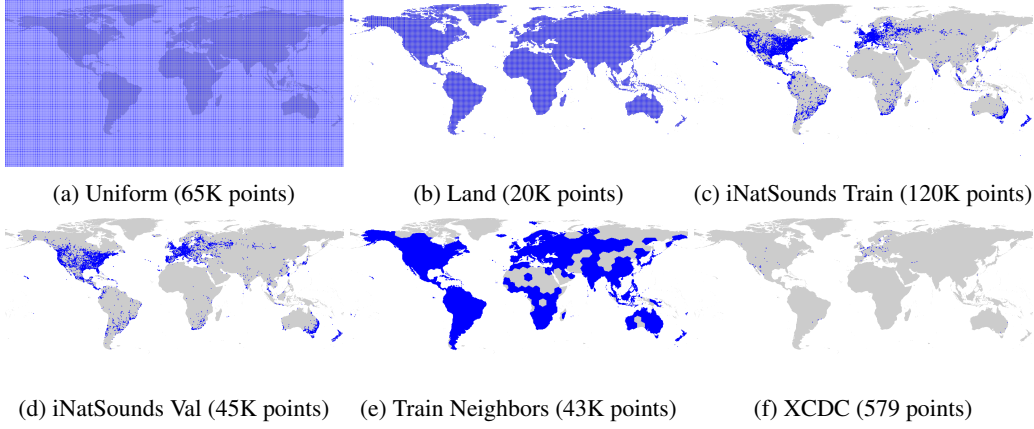


Figure A5: **Location Galleries.** Visualization of different galleries for evaluating geolocation.

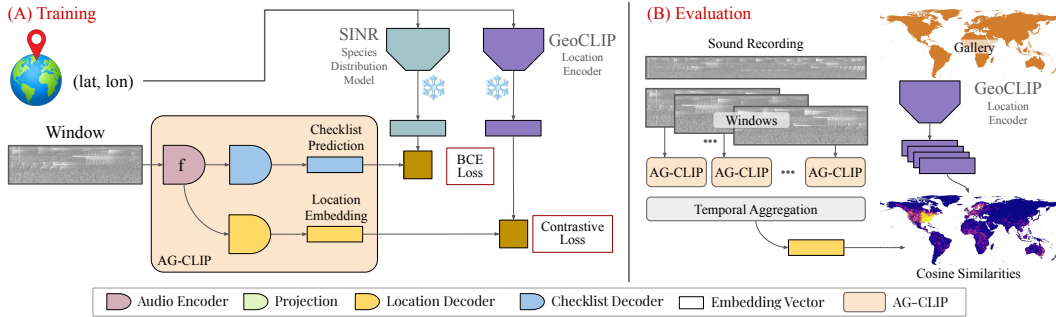


Figure A6: **Method Overview.** At training time (left), we sample a window uniformly at random from each audio recording. Features extracted by the audio encoder f_θ are fed to a checklist decoder which is used in a BCE loss with checklists given by SINR [17] as labels. Audio features f_θ are also fed to a location decoder, whose outputs are matched with corresponding GeoCLIP [60] location embeddings to get a contrastive loss. The full model is trained with the BCE loss and Contrastive loss. At test time (right), we densely sample all windows from a recording, predict final location features via the full AG-CLIP model and then aggregate these features across windows to get a recording-level prediction. Finally, we compute the similarity of this feature with GeoCLIP embeddings of a gallery of candidate locations to pick the most similar, which is the geolocation prediction.

takes the 1280 dimensional embeddings and projects it to the checklist dimension. The checklist and location decoders are both 2 layer MLPs with hidden dimensions of 128. After these modifications, the increase in model parameters is modest, from 4.4M for GeoCLIP to 4.7M for AG-CLIP.

We initialize the audio backbones with pretrained weights for iNatSounds [7] species identification. We take a weighted sum of the BCE and contrastive losses, with a weight of 0.01 on the BCE loss, which reflects its magnitude relative to the contrastive loss. We train for 50 epochs with early stopping using the Nesterov accelerated SGD optimizer with a batch size of 128, weight decay of 10^{-5} , and learning rate linearly ramped from 10^{-3} to 10^{-2} over the first 5 epochs and then cosine decayed back to 10^{-3} over the remaining 45 epochs. These hyperparameters were chosen with the validation set released by iNatSounds. We report test set performance.

Baselines: GeoCLAP and TaxaBind. For GeoCLAP, we get aerial imagery from the location with Google Maps API (similar to SoundingEarth [32]), and use its image embedding as the location embedding in our retrieval setup. Instead of encoding the (lat, lon) coordinates directly with a model, we first get the corresponding aerial image, and embed this image with their image encoder. SoundingEarth, the dataset used by GeoCLAP also contains Google Maps images, and we match the zoom levels and image sizes with that dataset. We use their audio and image encoders off the shelf.

TaxaBind includes encoders for 6 different modalities, all embedding in the same shared space. We use their audio and location encoders directly, in a setup very similar to ours. Note that TaxaBind

Table A1: **Location Galleries.** Effects of the location gallery used for AG-CLIP. The same AG-CLIP model (pre-trained on iNatSounds) is given different galleries at test time to get these results.

Gallery	# Locs	City 25km	Region 200km	Country 750km	Continent 2500km
Uniform	65K	01.3	15.0	38.6	69.2
Uniform	260K	02.9	15.8	38.9	69.5
Land	20K	01.6	15.4	38.6	69.6
Train	137K	06.6	17.4	41.0	70.3
Train Neighbors	43K	03.1	16.1	39.3	69.9
Validation	45K	06.7	17.6	41.1	70.6
XCDC	576	00.7	07.4	28.7	65.7

does not actually use geotagged audio. It uses geotagged images and audio-image paired data, which are used to train location-image and audio-image encoders, respectively. Since all modalities share the same space, this training strategy allows us to do audio→location retrieval, which we use for geolocation.

A.6 Transformer to handle Variable Length

Models that can reason over time can potentially capture more interesting patterns. For longer recordings like those of XCDC, temporal analysis can allow a model to properly combine geographic cues from different species. Our default average pooling does this too, by way of a simple voting of different windows. We also explore if we can do better with a transformer.

We still remain in the late-fusion regime: geolocation features are predicted for each window independently and the transformer aggregates these predictions at the end. We do this with the training set so that the transformer takes in a sequence of predicted location features $N \times L$ and then predicts a single L -dimensional feature, where L is the embedding dimension of the location encoder, which in our case is 512 for GeoCLIP. For easier batch construction, we keep the sequence length N fixed at 32, padding or cropping appropriately. Note that this corresponds to around 50s of audio. We use 6 transformer layers, each with 8 heads and a hidden dimension of 128. Only the transformer layers are trained and the CNN backbone is kept frozen. We use Adam with learning rate of 10^{-3} , weight decay of 10^{-3} , and train for 50 epochs.

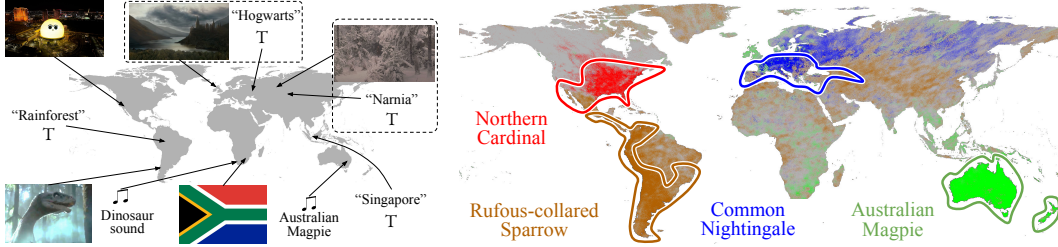
A.7 Ablation on Location Galleries

We present ablations on the location gallery in Table A1. We first experiment with galleries constructed by uniformly sampling points on the 2D world map (latitude, longitude). We sample locations in intervals of either 1° , leading to 65K locations, or 0.5° , leading to 260K locations. We obtain similar performances for both, with region level at 13.4% and 14.8%, respectively. This indicates that adding additional locations on a uniform grid may not improve performance much, but will lead to much higher compute. Next, we again sample uniformly (1° interval), but restrict locations to only land mass. Since the earth is only about 29% land, we are left with 20K locations, but performance does not change much, and actually improves slightly for some levels (city, region, and continent). This hints at the potential of smaller, but more targeted galleries.

Next, we use the train and validation sets to construct the gallery. Keeping the locations from each geo-tagged audio in the train set, we are essentially following the distribution of the dataset itself. Regions where recordings are dense in the training set have more locations in the gallery and conversely, sparse regions in the train set are allocated fewer gallery locations. If the test location distribution is similar to the train, this would be a good gallery, well balanced between granularity and compute cost. We could use the validation set instead to construct the gallery, although the train set is a more natural choice. Compared to the land gallery, we see small improvements at the continent and country level, but much bigger improvements at the region (16.4% vs 13.8%) and city (6.5% vs 1.3%) levels. The train neighbors gallery consists of uniformly sampled points like the uniform gallery, but only from H3 [5] hexagons that contain at least one training recording. This allows denser sampling

Table A2: **Geolocation on XCDC.** Models trained on iNatSounds training set and evaluated on XCDC.

Experiment		↓ Median Error (km)	↑ City 25km	Region 200km	Country 750km	Continent 2500km
Naive	Rnd Train Loc	9915 ± 99	00.0 ± 0.0	00.1 ± 0.2	00.5 ± 0.4	03.6 ± 0.5
Species Ranges	True Species Predicted Sp (All)	449 ± 06 1097 ± 18	00.5 ± 0.2 00.1 ± 0.1	25.8 ± 1.4 02.5 ± 0.3	68.8 ± 1.4 27.6 ± 1.1	99.0 ± 0.1 80.0 ± 0.3
Classify	Hierarchical	1116 ± 60	00.0 ± 0.0	05.3 ± 0.1	31.7 ± 1.9	69.7 ± 0.6
Retrieve	AG-CLIP (ours) AG-CLIP (XCDC gallery)	1112 ± 93 912 ± 72	00.2 ± 0.2 05.9 ± 0.2	04.3 ± 0.7 11.6 ± 0.7	26.3 ± 3.5 36.6 ± 3.1	71.9 ± 0.2 73.8 ± 0.3



(a) **Multimodal Geolocation.** Here, we explore geolocation using audio, images, and text. We try out some fun experiments and see what the geolocation models predict for these inputs. For some of these prompts like “Narnia” or Dinosaur sounds, we do not know what the correct location should be, but it is interesting to see what the model predicts.

(b) **Soundscape Affinities of Species.** Heatmaps of cosine similarity between the average soundscape embedding of selected species and a gallery of location embeddings sampled globally. High similarity regions (darker areas) indicate locations with soundscapes that match the species’ vocal features, showing alignment with known ranges and highlighting unexpected affinities with acoustically similar environments beyond typical habitats.

Figure A7: Additional experiments and visualizations

with a better control over the total number of locations. Even with 0.5° intervals, the number of locations drops to 43K, at the cost of slightly worse performance.

A.8 Audio Geolocation on XCDC

We report repeated runs with mean and standard deviations for XCDC experiments in Table A2. Standard deviations are relatively low. We also include an experiment with AG-CLIP where we use the XCDC-gallery instead of iNatSounds. We see a good boost in performance, particularly at finer scales. However, these improved results are still worse than iNatSounds, supporting our hypothesis about the difficulty of our models to identify species rich data in XCDC.

A.9 Additional Details for Multimodal Geoforensics

We use YouTube clips for each movie shot we investigate. Searching for the moment where we suspect a discrepancy (based on viewer comments), we extract 10s audio clips and take a screenshot. The audio is geolocated by AG-CLIP. For the image, we use CLIP image encoder, followed by a (frozen) projection, as done by GeoCLIP. We visualize geolocation predictions of each modality of each example by arrows. These arrows show only the approximate location, but we compute the discrepancy errors exactly.

GeoCLIP keeps their image encoder frozen and trains a location encoder. This allows them to swap in CLIP’s text encoder instead of image, facilitating geolocation of text. Text descriptions of visual or acoustic scenes can serve as another modality for geoforensics.

A.10 Multimodal Geolocation

In AG-CLIP, we keep the location encoder frozen from GeoCLIP, who in turn had kept their image encoder frozen from CLIP. Thus, we have a set of encoders that embed audio, location, images and

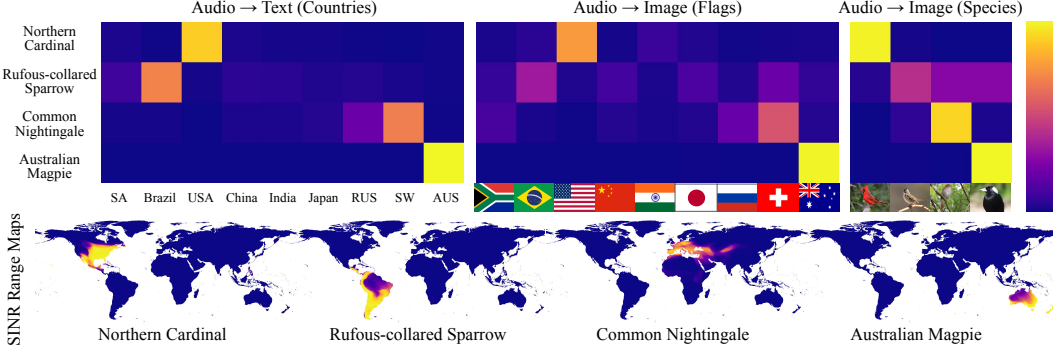


Figure A8: **Multimodal Retrieval.** We visualize some examples for Audio → Text and Audio → Image retrieval. We use the same average soundscape embeddings of species shown in Fig. A.11 and retrieve some text or image queries. We show similarity matrices for 1) Country names as text, 2) Country flags as images and 3) Same species as images. Retrieval for country texts and flag images are relatively consistent. For species image retrieval, we see some confusion for the Rufous-collared sparrow, but all species are correctly matched. At the bottom, we show the SINR range maps of these species for context of the countries these species are typically found in.

text to the same space, allowing us to do multimodal geolocation (see Fig A7a). Interestingly, CLIP can recognize flag images as well, and can geolocate them to the correct countries. The Las Vegas sphere (top left) finished construction after these models were trained, but they are interestingly still able to geolocate it accurately, perhaps because of some background details.

Text helps expand the scope of queries in this problem. We can ask the model to geolocate the text “rainforest”, and it predicts a location close to the Amazonas, the biggest rainforest in the world. Giving country names as text queries also seems to work well. As fun experiments, we also ask the model to geolocate fictional places like “Hogwarts” and “Narnia.” For Narnia, the model predicts a location near Russia, which may be due to the snowy and mountainous landscapes seen in the first part of the movie. Image geolocation on a video frame from the movie also points to a similar location. Similarly for Hogwarts, the predicted locations of text and image geolocation models are interestingly close. While we cannot say whether the predicted geolocations for these are correct or not, it can be a fun way to probe what these models are learning.

A.11 Soundscape Affinities of Species.

How does the soundscape associated with a species relate to its geographic range? We explore this question using AG-CLIP and visualize the results in Fig. A7b. For each species, we compute the average audio embedding using test recordings from iNatSounds associated with that species. We then calculate the cosine similarity between this average embedding and a gallery of location embeddings uniformly sampled across the globe (restricted to land locations). The similarities are clamped to the range $[0, 1]$ and used as the alpha channel in the heatmap visualizations.

Fig. A7b shows results for four species: Northern Cardinal, Rufous-collared Sparrow, Common Nightingale, and Australian Magpie, alongside coarse approximations of their range maps. The soundscape embedding of the Northern Cardinal aligns well with its range, but interestingly, it does not capture the western portion of its range as strongly, possibly reflecting the distinct soundscapes of eastern forests versus western deserts. For the Rufous-collared Sparrow, the soundscape feature extends far beyond its range in South America, likely due to its occupancy of semiopen habitats (i.e., villages, towns, and farmland), making it acoustically similar to many locations worldwide. The Common Nightingale’s soundscape affinity stretches into Russia, suggesting a similarity in soundscapes between northern Europe and parts of Russia. Finally, the Australian Magpie’s embedding aligns with its range in Australia and New Zealand but also shows unexpected affinities with deserts in Africa and rainforests in Southeast Asia, two habitats present in Australia.

These results highlight that the soundscape features learned by AG-CLIP capture both expected and surprising affinities of species soundscapes, providing insights into the relationship between species vocalizations and the broader acoustic environment.

A.12 Retrieving Images and Text from Audio

Since we embed audio in a shared text-image-location feature space, we can use our geolocation models to perform Audio → Text and Audio → Image retrieval by simply replacing location embeddings with the corresponding modality. We present a few such experiments in Fig A8.

We use the same average soundscape embeddings of species shown in Fig. A.11. We compute similarities of these embeddings with certain text or image embeddings for retrieval. First we attempt Audio → Text by comparing each species feature with text features of country names. Notably, we observe some confusion between Switzerland and Russia for the Common Nightingale. These similarities closely reflect the SINR [17] species range maps for corresponding species seen at the bottom of the figure. Next, we attempt Audio → Image by using images of flags of the same set of countries. We observe predictions very similar to the Text retrieval experiment, which underscores how well these modalities are paired. Finally, we repeat the Audio → Image experiment by using species images instead of flags. While there is some confusion for the Rufous-collared Sparrow, the other three species are surprisingly confident and the model retrieves all species correctly. Some multimodal retrieval tasks are often constrained by the availability of paired data from each modality. These experiments show a promising and flexible alternative of using “weakly” paired data where some but not all modalities are paired with each other.

A.13 Compute Resources

We used a single A100 GPU with 80 GB GPU memory for all experiments. On a node with 1 GPU and 8 CPUs, one experiment of AG-CLIP takes 2.5 hours on iNatSounds (training + testing) and about 20 minutes for XCDC (testing only). Other approaches of species oracles, naive baselines and species ranges are much faster. Classification and regression take about the same training time as AG-CLIP, and are faster at inference time since retrieval methods need location galleries to get prediction.